Title

Toward a unified connectomic target for deep brain stimulation in obsessive-compulsive disorder

Authors

Ningfei Li[1*], Juan Carlos Baldermann[2], Astrid Kibleur[3,4], Svenja Treu[5], Gavin J.B. Elias[6], Alexandre Boutet[6,7], Andres M. Lozano[6], Stephan Chabardes[3], Veerle Visser-Vandewalle[8], Mircea Polosan[3,9,10], Jens Kuhn[2,11], Andrea A. Kühn[1], Andreas Horn[1]

1. Movement Disorders & Neuromodulation Unit, Department for Neurology, Charité University Medicine Berlin, Germany.
2. Department of Psychiatry and Psychotherapy, University of Cologne, Medical faculty, Cologne, Germany.
3. Univ. Grenoble Alpes, F-38000 Grenoble, France.
4. OpenMind Innovation, F-75008 Paris, France.
5. Laboratory for Clinical Neuroscience, Centre for Biomedical Technology, Universidad Politecnica de Madrid, Spain.
6. University Health Network, Toronto, Ontario, Canada.
7. Joint Department of Medical Imaging, University of Toronto, Ontario, Canada
8. Department of Stereotactic and Functional Neurosurgery, University of Cologne, Cologne, Germany.
9. Inserm, U1216, Grenoble Institut des Neurosciences, F-38000 Grenoble, France.
10. Psychiatry Department, CHU Grenoble Alpes, F-38000 Grenoble, France.
11. Johanniter Hospital Oberhausen, EVKLN, Department of Psychiatry, Psychotherapy and Psychosomatics, Oberhausen, Germany.

* **Corresponding Author**

Ningfei Li
Department of Neurology, Movement Disorders and Neuromodulation Unit, Charité - University Medicine (CCM), Berlin, Germany.
E-mail: ningfei.li@charite.de

Abstract

Multiple surgical targets have been proposed for treating obsessive-compulsive disorder (OCD) with Deep brain stimulation (DBS). However, different targets may lie along the same fiber bundle, which could be responsible for clinical improvement. Here we analyzed data from two cohorts of OCD patients that underwent DBS to either the anterior limb of the internal capsule (ALIC) or the subthalamic nucleus (STN). Fiber tracts that were predominantly connected to electrodes in top or poor DBS responders – based on improvement on the Yale-Brown Obsessive-Compulsive Scale (Y-BOCS) – were isolated and each assigned a predictive value. Strikingly, the same fiber bundle that was positively discriminative of treatment response emerged in both cohorts, independently from each other. Using this tract, it was feasible to cross-predict clinical improvement across DBS targets, cohorts and centers. Our results suggest that obsessive-compulsive symptoms could indeed be modulated by stimulation of this specific bundle and demonstrate that connectomics-derived improvement models informed by patients operated in one target may predict outcome in patients operated in an alternative target.

Obsessive-compulsive disorder is a debilitating disease with a life-time prevalence of around 2%. Treatment of severe cases by deep brain stimulation (DBS) to the anterior limb of the internal capsule has been approved by the FDA (Humanitarian Device Exemption) in 2009. A variety of other targets have been proposed, however, including the STN [1,2], ALIC [3], nucleus accumbens (NAc) [4–6], ventral capsule/ventral striatum (VC/VS) [7], inferior thalamic peduncle (ITP) [8,9], bed nucleus of the stria terminalis (BNST) [10], anteromedial globus pallidus interna (amGPi) [11], superolateral branch of the medial forebrain bundle (slMFB) [12] and medial dorsal and ventral anterior nucleus of the thalamus (MD/V ANT) [13] (for an overview of targets see [14]). A recent prospective clinical trial implanted four electrodes per patient with one pair in the STN and one in the ALIC [15].

In parallel, DBS has experienced a conceptual paradigm-shift away from focal stimulation of specific brain nuclei (such as the subthalamic nucleus in Parkinson's Disease; PD) toward modulating distributed brain networks (such as the motor basal-ganglia cortical cerebellar loop in PD) [16–18].

Thus, it could be possible that, of the multiple targets proposed, some or most may in fact modulate the same treatment network to alleviate symptoms. Such a concept has been proposed in the past by Schlaepfer and colleagues for the case of treatment-refractory depression [19]. According to their concept, the supero-lateral branch of the medial forebrain bundle may connect most if not all surgical targets that have been proposed for treatment of depression (e.g. subgenual cortex, ALIC, NAc, habenula). In a recent study, it was further implied that smaller distances to the slMFB were associated with better clinical improvement in OCD patients implanted for ventral ALIC-DBS, even though the anatomical position of the electrodes themselves were not related to treatment response [20]. Thus, in theory, the *tract itself* could be a surgical target – and it could be modulated in a similar way when targeting various points along its anatomical course. This concept may seem oversimplified given the extensive complexity of the human brain and the potential complexity of each structure's function. Still, even older invasive therapies, such as cingulotomy and capsulotomy primarily aimed at disrupting connectivity to frontal regions by lesioning white matter bundles [21]. Moreover, it was recently shown that such tract- or network-based concepts could be used to predict clinical improvement across DBS centers and surgeons for the case of Parkinson's Disease [17]. Using modern neuroimaging methods and high-resolution connectomic datasets, it could be shown that connectivity of the DBS electrodes to specific cortical regions is associated with stronger therapeutic effects in various diseases treated with the surgical procedure [17,22–25].

For the case of OCD, Baldermann and colleagues have recently demonstrated that structural connectivity from DBS electrodes to medial and lateral prefrontal cortices were associated with stronger symptom alleviation [22]. Crucially, they were also able to identify a specific subsection of the ALIC that was highly associated with symptom improvement after one year of DBS. Of note, connectivity to this fiber tract was able to predict ~40 % of the variance in clinical outcome of this sample. Already in their study, the bundle was described to connect to both the medial dorsal nucleus of the thalamus (which has received substantial attention in the context of OCD) and to the anterior part of the STN. The STN itself is a prominent target for DBS of various diseases including PD [26], dystonia [27], OCD [28] and Tourette's Syndrome [29]. The small nucleus receives wide-spread connectivity from most parts of the prefrontal cortex and is involved in motor, associative and limbic processing [30]. Likely due to these cortico-subthalamic projections, the nucleus has various functional zones that largely follow the organization of the frontal cortex, i.e. the sensorimotor parts of the STN are posterior and are followed by pre-/oculomotor-, associative and limbic domains in anteromedial direction.

Consequently, the anterior (associative/limbic) parts of the STN have been targeted by DBS for OCD [28]; these same subregions were also exclusively connected to the tract-target identified by Baldermann and colleagues in ALIC-DBS patients [22]. Following up on this, our study aimed at testing whether the same tract may be associated with good clinical outcome in a cohort treated with STN-DBS. Thus, here, we retrospectively analyzed two cohorts of DBS patients that were treated with either STN-DBS or ALIC-DBS in order to test our hypothesis, that the same tract could potentially predict clinical improvement in STN-DBS as well as ALIC-DBS.

Results

Patients in both cohorts were of similar age with a similar Y-BOCS score at baseline (see table 1 for demographic details). Y-BOCS improvement was also comparable across groups (9.6 ± 6.5 points or 31.0 ± 20.5 % in the ALIC cohort vs. 13.8 ± 10.8 points or 41.2 ± 31.7 % in the STN cohort).

Table 1: Patient demographic details and clinical results of the two cohorts

	ALIC **DBS Cohort (Mean ± SD)**	STN **DBS Cohort (Mean ± SD)**
Center	**University Hospital Cologne**	**University Hospital Grenoble**
Reference(s)	(22, 31)	(28)
N (females)	22 (12)	14 (9)
Age	41.7 ± 20.5	41 ± 9
Y-BOCS Baseline	31.3 ± 4.4	33.4 ± 3.7
Y-BOCS 12 months after DBS	20.7 ± 7.7	19.6 ± 10.6
Absolute Y-BOCS Improvement	9.6 ± 6.5	13.8 ± 10.8
% Y-BOCS Improvement	31.0 ± 20.5 %	41.2 ± 31.7 %

Electrode localization confirmed accurate placement to each of the two target regions for all patients (Figure 1).

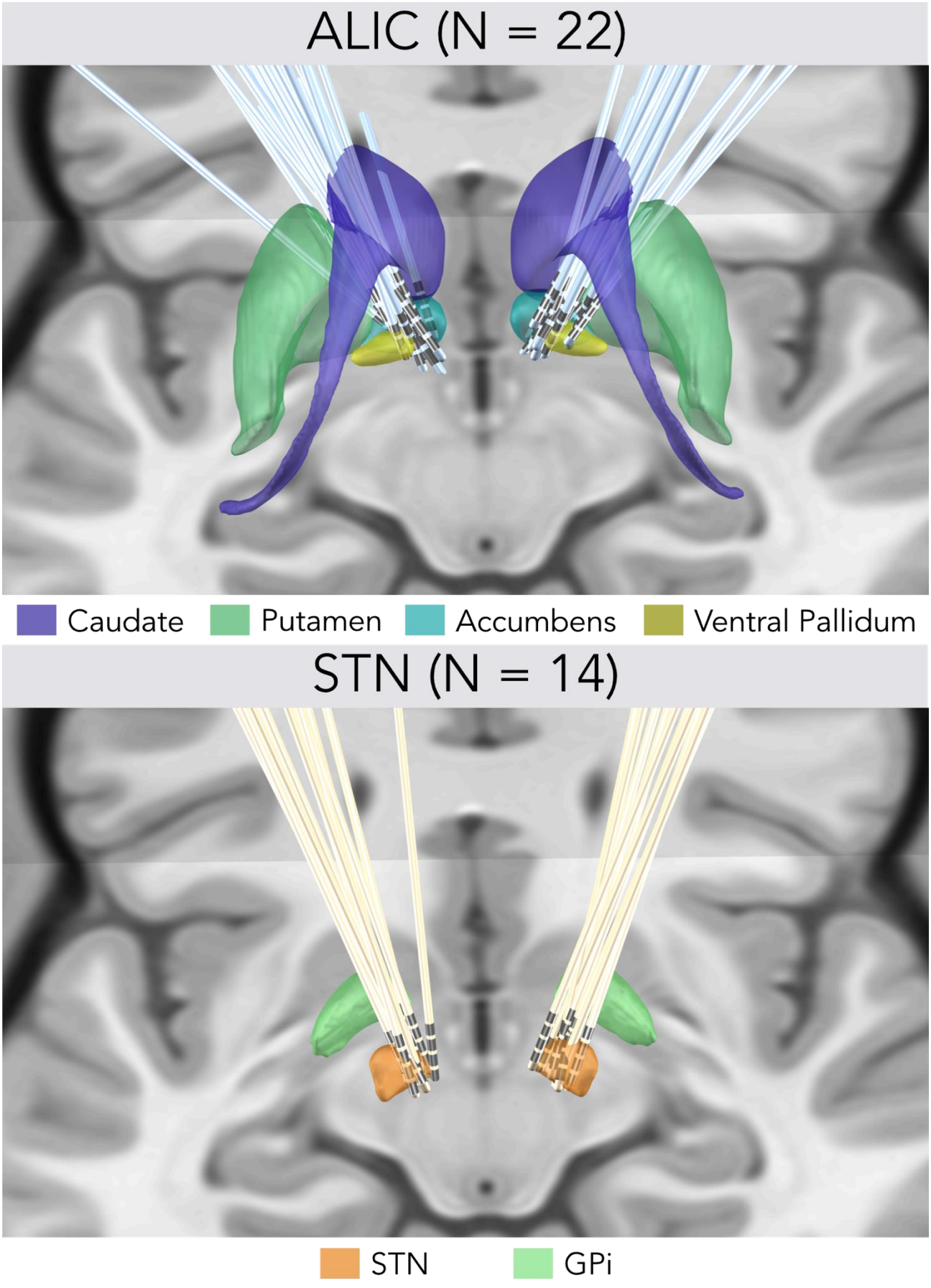

Figure 1. Overview of the lead electrodes placements of both ALIC DBS and STN DBS cohorts. Subcortical structures defined by CIT168 Reinforcement Learning Atlas [31] (ALIC cohort) and DISTAL Atlas [32] (STN cohort), with coronal and axial planes of the T1-weighted ICMB 152 2009b nonlinear

template [33] as background.

Connectivity analysis results based on the N = 985 HCP normative connectome are shown in Figure 2. The overall connectivity of electrodes to other areas in the brain (without weighing for clinical improvement) was strikingly different between the two cohorts (Figure 2, top row). This is hardly surprising given it mainly reflects the overall structural connectivity profiles of the two DBS targets and the STN as a widely connected basal ganglia entry point and the ALIC as a white matter target are overall differently connected in the brain. However, when tracts were weighted by their ability to discriminate between top and poor responders (T-score method, Figure 6), a bilateral positively discriminative tract to the medial prefrontal cortex emerged that was shared by both cohorts (Figure 2, middle row). The degree of lead connectivity to this tract correlated with clinical improvement ($R = 0.56$ at $p = 0.006$ in the ALIC cohort and $R = 0.64$ at $p = 0.014$ in the STN cohort; Figure 2, bottom row).

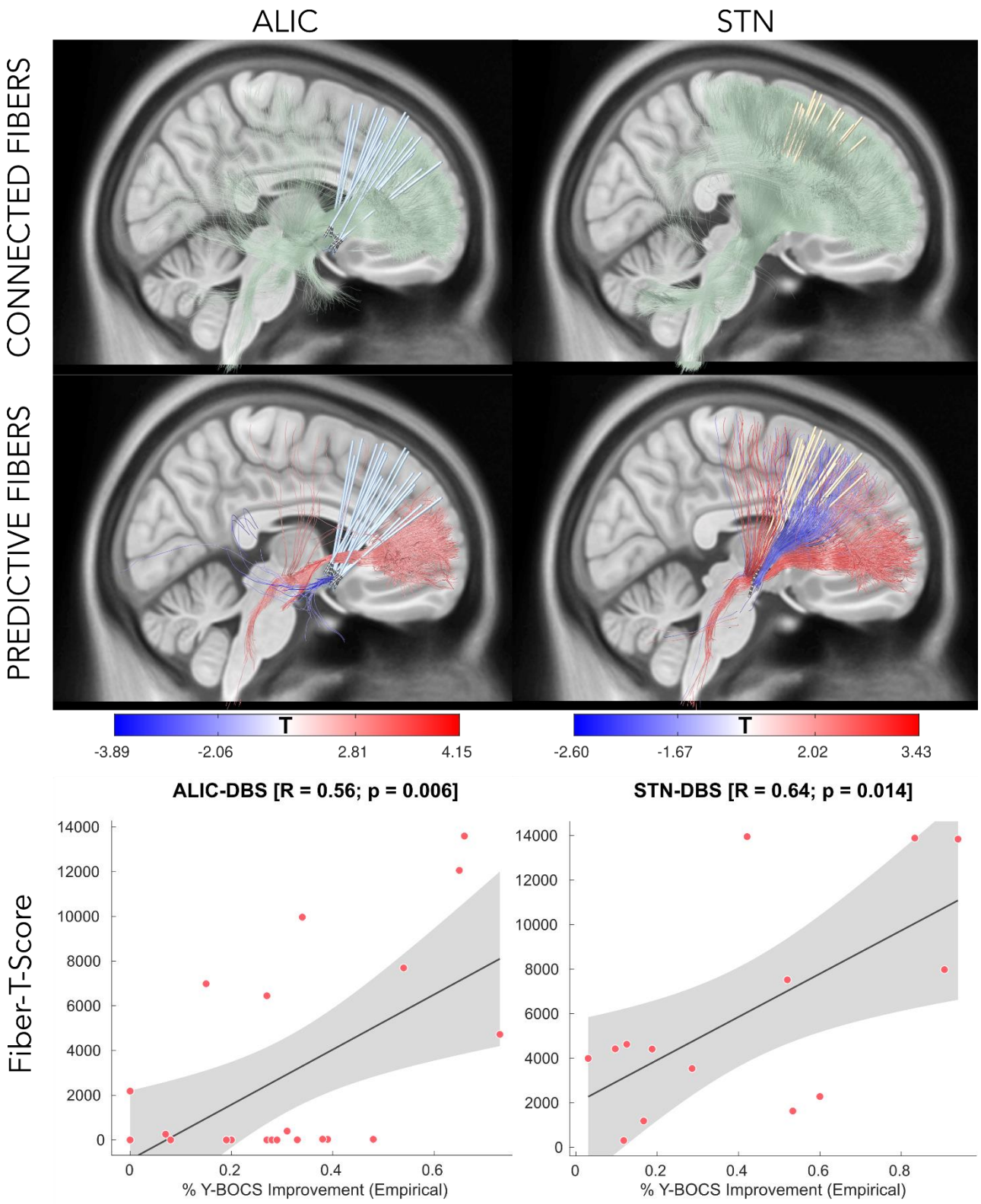

Figure 2. Structural connectivity of the VTA. All fibers traversing the VTA are shown in green (top row) as connected fibers. Predictive fibers positively correlated with clinical improvement are shown in red, while those negatively correlated with clinical improvement are shown in blue (mid row). The top and bottom 20% (based on fiber T-scores) of the predictive fibers are shown. Correlations between the degree of connectivity to predictive tracts (sum of aggregated fiber-T-scores under each VTA) and the clinical improvements are shown in the bottom row.

When performing the same analysis on all patients (of both cohorts together), the same tract emerged even more clearly (Figure 3 top). Stated differently, this tract shown in red color was able to discriminate between top and poor responders, statistically. Thus, patients with good improvement in both groups were more likely to be connected to the tract while non- or poor responders were likely not or only weakly connected to the tract. The tract passed slightly dorsal to the group of electrodes of the ALIC-cohort and coursed centrally or slightly ventral to the electrodes of the STN cohort. To quantitatively verify if the same fiber tract could be associated with clinical improvement in both cohorts, we first correlated the degree of connectivity of each cohort with this tract (i.e. how much VTAs "activated" the tract, expressed by the sum of T-values of fibers connected to the tract). This revealed a significant correlation ($R = 0.48$ at $p = 0.003$; Figure 3 bottom left). Subsequently, we estimated the optimal tract exclusively based on the ALIC cohort (as it is shown in figure 2 middle left) and predicted improvement of the STN cohort and vice versa (i.e. using the tract as it is shown in figure 2 middle right based on the STN cohort to predict outcome in the ALIC cohort). Results of this cross-prediction across DBS centers and targets is shown in figure 3, bottom right ($R = 0.37$; $p = 0.027$).

This final bundle may indeed represent a "tract-target" for to treat OCD with DBS. Given this potential clinical importance, we characterized its anatomical properties using additional views relatively to anatomical landmarks that could be used during stereotactic planning (Figure 4). We also released this tract as an atlas in stereotactic (MNI) space within Lead-DBS software (www.lead-dbs.org), where it could theoretically be used to guide DBS programming in existing patients (see video S1 for example usage). Of note, Lead-DBS is scientific and not clinical software but given the experimental nature of OCD-DBS (i.e. most patients are enrolled in clinical studies), we deemed such an openly-available tract atlas potentially useful.

Our tract may potentially "unify" some aspects of the STN and ALIC targets for OCD. In a final analysis, we aimed at setting it into synopsis with other DBS targets that have been used in the OCD context in the literature. Using a novel method to convert stereotactic coordinates into MNI space in a probabilistic fashion [34], we converted literature-based targets and visualized them in synopsis with the discriminative fiber tract identified in the present study (see figure 5 and table 2). Of note, a large number of all available DBS targets for OCD seemed to cluster on or around the anatomical trajectory of the tract identified in the present study.

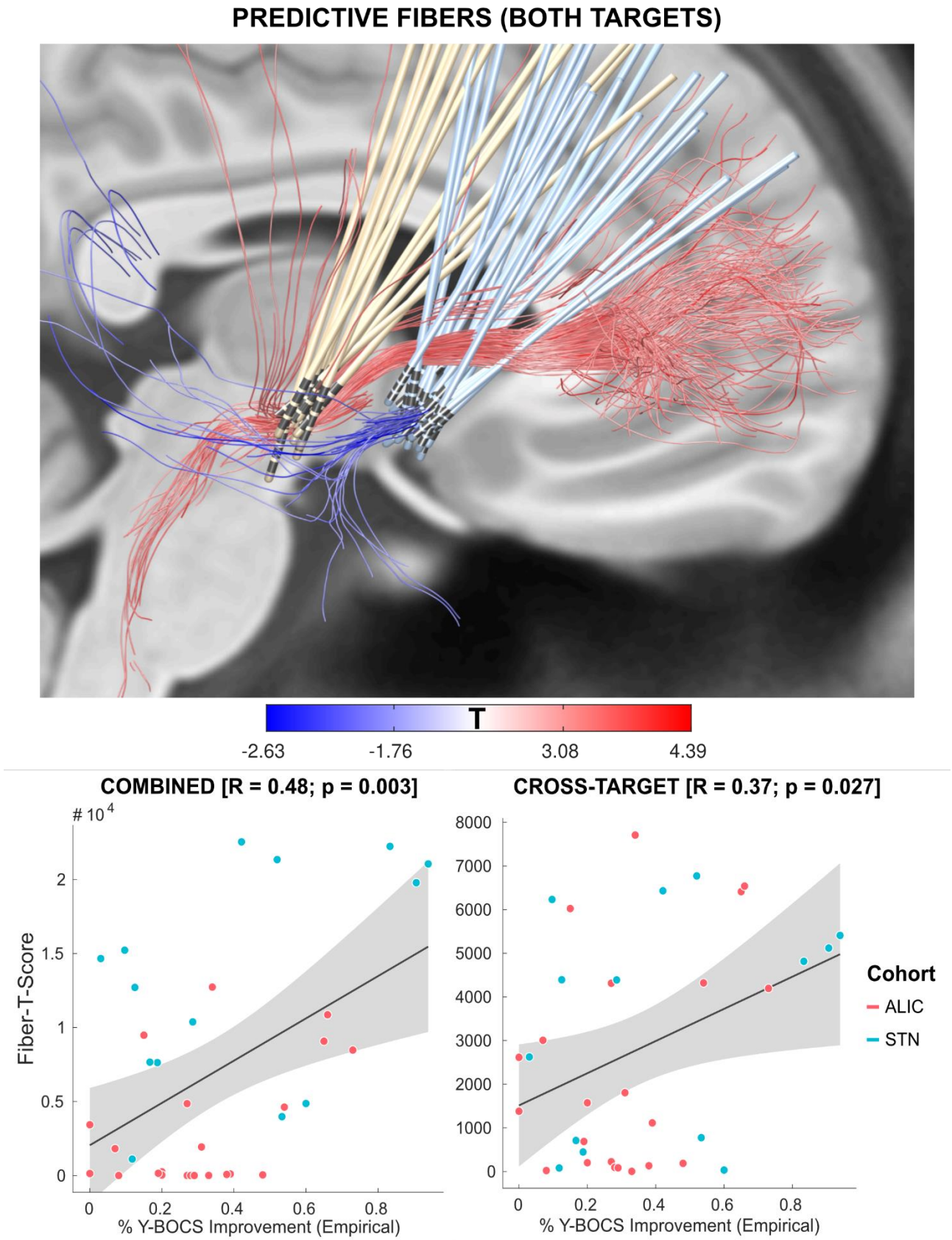

Figure 3. Common predictive fibers for both targets (top). The sum of aggregated fiber-T-scores under each VTA explained % Y-BOCS improvement (bottom left). Moreover, the tract defined in one target could cross-predict improvement in the cohort treated with the other target (bottom right). Red fibers are positively associated with clinical improvement, blue fibers negatively.

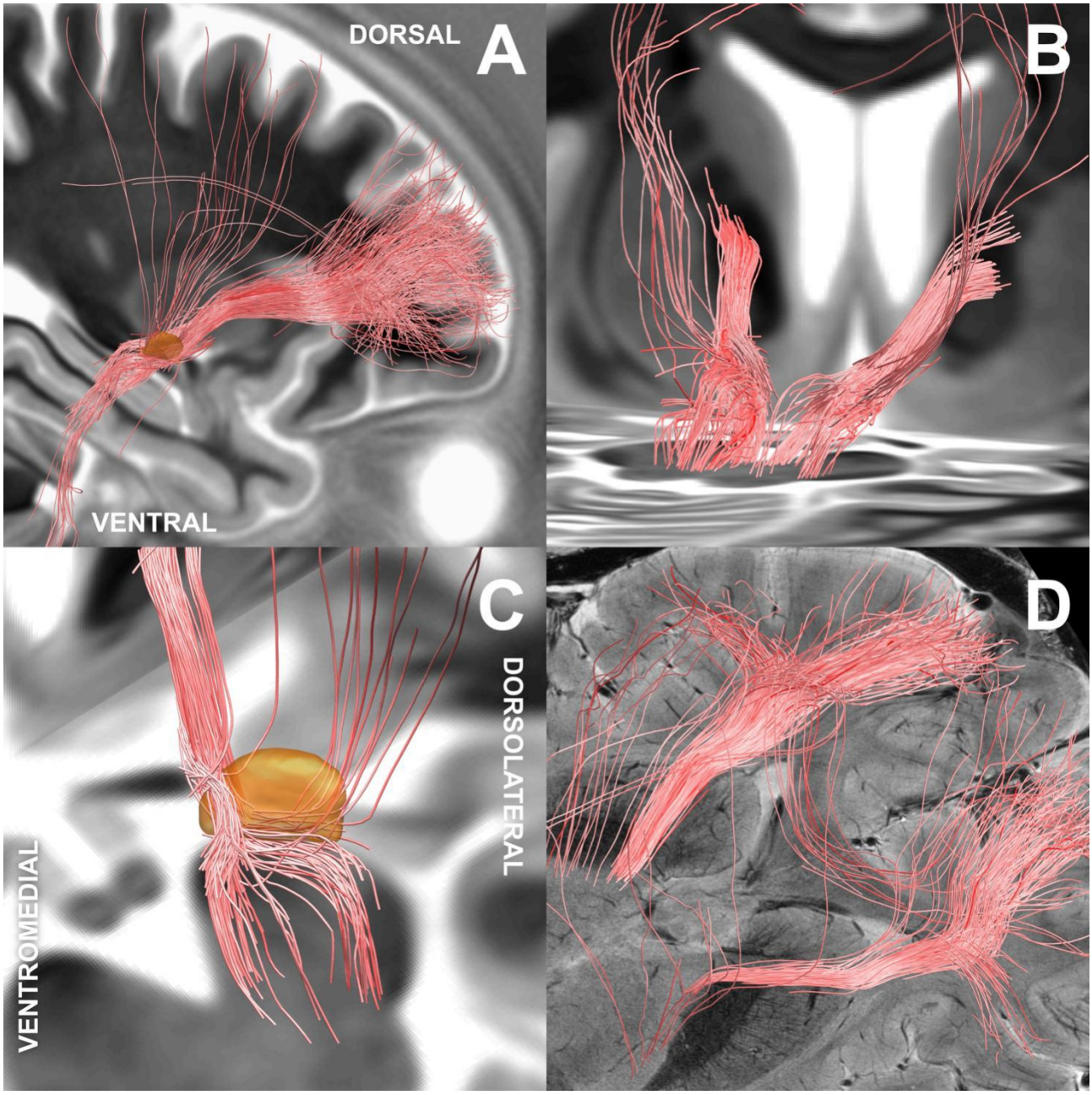

Figure 4. Positively predictive fiber tracts that were commonly discriminative in both ALIC- and STN-cohorts shown from multiple angles to further characterize them, anatomically. A) Sagittal overview with STN in orange. B) Trajectory within the internal capsule while it passes putamen and caudate. C) Close-up showing the tracts course within and below the anterior STN. D) Oblique view of the axial aspect after entering the anterior limb of the internal capsule coming in from ventrally.

Table 2: DBS targets for treatment of OCD based on literature results. *MD*, medial dorsal thalamic nucleus; *VA*, ventral anterior thalamic nucleus; *iml*, internal medullary lamina; *MCP*, mid-commissural point; *AC*, anterior commissure
* Tourette patients, with prominent symptoms of OCD

DBS Target	Reference	Number of patients	% YBOCS change	AC/PC coordinates	Relative to	Target type	MNI coordinates (fig. 6)
STN	Mallet et al. 2008 [35]	8	32.14	NA	AC	Tip of the electrode	±11.30 -9.90 -7.81
amGPi	Nair et al. 2014 [11]	4*	NA	±14.47 9.85 -3.28	MCP	Tip of the electrode	±15.66 -1.41 -8.22
VC/VS	Tsai et al. 2010 [36]	1	NA	±7.5 16.3 -3.05	MCP	Tip of the electrode	±7.92 5.51 -9.01
slbMFB	Coenen et al. 2017 [12]	2	41.7 at 12 months	±7.6 -1.72 -3.0	MCP	Active contacts	±8.35 -13.64 -7.00
NAc	Sturm et al. 2003 [4]	4	NA	±6.5 2.5 -4.5	AC	Tip of the electrode	±6.98 3.69 −10.55
ALIC	Nuttin et al. 2003 [37]	6	38.69	±13 3.5 0	AC	Tip of the electrode	±13.84 5.17 -5.04
MD	Maarouf et al. 2016 [13]	4	0	±4.7 18.52 4.87	AC	Active contacts	±4.89 21.51 -1.37
VA				±6.84 13.76 7.78			±6.70 16.85 2.76
iml				±5.78 14.9 7.08			±5.70 17.96 1.77
ITP	Lee et al. 2019 [9]	5	52	±6.5 -3 -0.5	AC	Tip of the electrode	±6.92 -1.84 -5.13
BNST	Nuttin et al. 2013 [38]	4	NA	±6 0 0	AC	Tip of the electrode	±6.33 1.39 -4.87

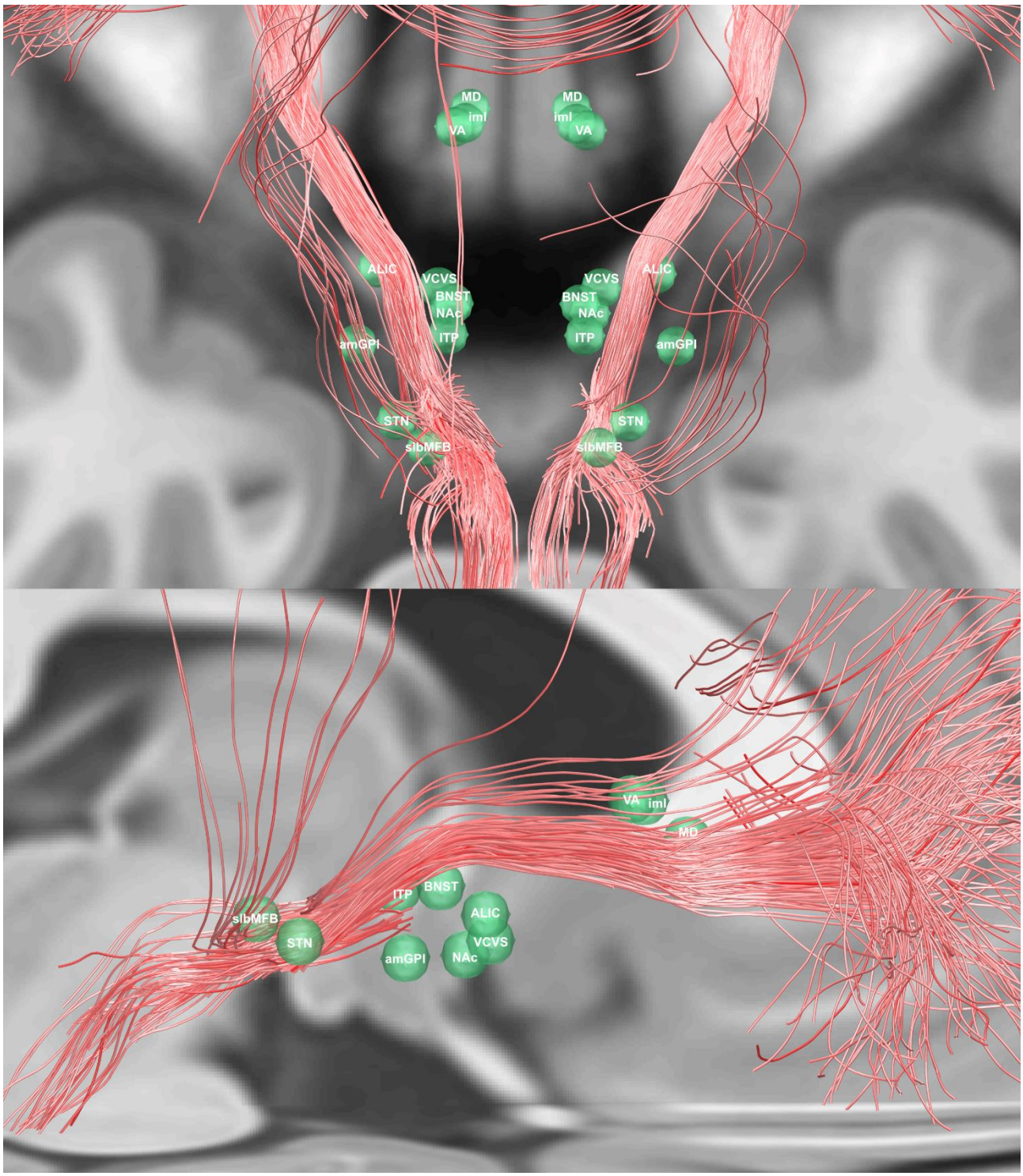

Figure 5. Overview of the positively predictive fiber tracts identified in the present study in synopsis with DBS targets for treatment of OCD based on literature results that were mapped to MNI space.

Discussion

In the present work, we analyzed data from two cohorts of OCD patients with different DBS targets using a connectomic approach. Strikingly, in both ALIC-DBS and STN-DBS, the same fiber bundle, which connected the group of VTAs with the medial prefrontal cortex, was predictive of good clinical improvement. It was possible to cross-predict clinical improvement based on the degree of how strongly the tract was activated in patients across DBS cohorts, targets and centers.

In recent work by Baldermann et al. 2019 [22], a fiber bundle was identified that was associated with good clinical improvement in OCD when modulated by high-frequency DBS. This bundle connected the medial and lateral prefrontal cortex, subthalamic nucleus and MD nuclei of the thalamus in ALIC-DBS patients. Baldermann and colleagues concluded that DBS would modulate the prefronto-subcortical communication within this fronto-thalamic pathway, which is in line with the assumption that a dysregulation in the fronto-striato-thalamic circuit underlies OCD [39–41]. This linkage was further supported by a recent study, showing enhanced cognitive control and theta increases in the medial and lateral PFC after VC/VS DBS in patients with MDD and OCD [42]. Besides, these changes in frontal oscillations were able to predict clinical outcome. However, as many targets have been used clinically in OCD [14], it is still unclear which target is best and whether the underlying stimulated networks are the same. Highly relevant to the present work, Tyagi et al. [15] recently reported results from a prospective clinical trial in which patients with OCD (N = 6) received electrodes to *both* the STN and ALIC targets that are discussed here. For the first 12 weeks, patients were stimulated at one target site in a randomly assigned and double-blind fashion. Then, patients were switched to the other target for another 12 weeks. Finally, an open-label phase, in which both sets of electrodes were switched on, followed. Needless to say, such a direct double-blinded and prospective head-to-head comparison is ideally suited for comparing the two targets. In line with our results, Y-BOCS improvement in this trial was not significantly different for either target in the Tyagi study and, similar to our findings, striking differences in average connectivity profiles (without clinical weighing) were found between the two targets (see Figure 2, top row). Tyagi et al. then moved on to conclude that different networks are stimulated when stimulating the two targets since improvements in depressive symptoms were stronger in the ALIC target while cognitive inflexibility symptoms improved more strongly in the STN stimulation phases. These results do not contradict the findings of the current study since we exclusively focused on Y-BOCS score improvements (additional but corresponding scores above and beyond the Y-BOCS score were not available for the

cohorts studied here). Hence, our findings – that the two DBS targets may exert their clinical utility towards OCD symptoms by potentially modulating the same tract – should not be misinterpreted as if the two were fully equivalent or even exchangeable targets. As Tyagi et al. demonstrated, it may indeed matter to choose between the two targets based on other symptoms each patient may have – depending on depressive or cognitive inflexibility symptoms, rather than properly obsessive or compulsive symptoms.

Toward symptom-specific circuitopathies

When integrating the results of Tyagi et al. and our present results, it seems that two testable hypotheses with implications beyond the STN and ALIC and above and beyond OCD may be proposed. First, based on the joint results of both studies, it seems that (two) different surgical targets may reduce *the same* symptoms equally well – potentially by modulating the same tract or network. Second, it seems that different surgical targets may modulate not only one (shared) network but other networks that are not shared (widely different connectivity profiles of the two targets shown by both studies and differential effects on depressive and cognitive functions described in the Tyagi et al. study). From these two observations, one may derive the concept of symptom-specific networks that – when modulated – do not ameliorate a specific disease but rather specific symptoms that are present in the disease. In OCD, accordingly, different symptom types (for example contamination vs. checking) were found to activate different prefrontal sites (ventromedial vs. dorsolateral, respectively) [43]. Moreover, in another study combining a pre-surgical symptom provocation paradigm with patient-specific probabilistic tractography, these differential content-specific prefrontal activations predicted optimal contact positions along a dorsoventral striatal axis [44].

Similar observations have been made before in other diseases. For instance, Akram and colleagues demonstrated that connectivity to specific cortical regions is associated with improvement in different clinical features of Parkinson's Disease (e.g. connectivity to M1 preferentially reduced tremor while to the SMA reduced rigidity and bradykinesia) [23]. Another example is the involvement of a cerebello-thalamic pathway for tremor symptom alleviation in both PD and Essential Tremor [45,46].

Our study does not have the aim to analyze which surgical target is potentially better for treatment of OCD – the available clinical data and retrospective design are not well suited to answer this question. However, our study was able to predict symptom-specific clinical improvement *across DBS targets* based on connectivity data. Once more, the tract that our data seems to shape out is predictive for Y-BOCS improvement – but completely different

tracts could have emerged when repeating the analyses for depressive or cognitive flexibility symptoms (as analyzed by Tyagi et al.). Unfortunately, these data are not available for our cohorts. It is likely, that there the two targets do not share tracts that are predictive for improvement in these additional symptoms (e.g. depressive symptoms and cognitive flexibility).

Similar shared symptom networks could be present in different diseases in which various experimental surgical targets are being investigated. Major Depression and Tourette's Syndrome are obvious candidates and extensive work in this direction is currently ongoing [47–51]. Similar concepts could even be applied to more established targets such as STN vs. GPi DBS [52–54] or symptom-specific alleviations across diseases (e.g. tremor in Parkinson's Disease, Essential Tremor and Dystonic Tremor).

Following from this line of reasoning, it is possible that we are currently entering the era that will define symptom specific circuitopathies. Potentially, DBS surgery in the (distant) future could involve detailed preoperative phenotyping to establish a broad patient-specific symptom score. Based on databases of clinical improvements along the affected symptom axes, *a mix of networks* that could be modulated to alleviate each patient's symptoms could be identified. Finally, based on these, the optimal surgical target could then be calculated at the crossing sites of symptom networks for each specific patient.

Limitations

Several limitations apply for the current work. First and foremost, the retrospective character of the study is not ideal to compare and study effects of clinical outcome which is why we kept clinical information to a minimum and instead referred to clinical studies. Second, we used normative connectome data instead of patient-specific diffusion-weighted MRI data (which is unavailable for most of the patients included). Use of normative connectomes has been introduced in other clinical domains where patient-specific MRI data is unavailable, such as stroke [55–57] or transcranial magnetic stimulation [58]. In DBS, the technique has also been applied before and – as in the present study – has led to models that could be used to predict out-of-sample data [17,22,59]. In addition to the practical advantage of being applicable in cases where patient-specific data is lacking, normative data also has the theoretical advantage of much better data quality. In the present case, a connectome dataset was derived from a high N of 985 subjects scanned under research conditions by one of the best methodological groups in the world [60]. Data of such quality can usually not be acquired in individual patients and test-retest scan reliability in DBS settings has shown to be poor even when applying state-of-the-art MRI protocols [61]. Thus, the use of normative connectomes

may in fact constitute an advantage rather than a limitation, especially since we demonstrate its capability of out-of-sample predictions. Potentially, in the future, the use of mixed datasets that are informed by both normative (high N, high signal-to-noise) and individualized (patient-specific) datasets might be worthwhile to investigate.

Finally, slight inaccuracies in lead localization may result from the approach of warping electrodes into common space as done here. To address this issue, we used a modern neuroimaging pipeline that has been scientifically validated in numerous studies and involves advanced concepts such as brainshift correction, multispectral normalization, subcortical refinement steps [62] and phantom-validated electrode localizations [63]. The normalization strategy that was applied was found to automatically segment the STN as precisely as manual expert segmentations [64] and each step of the pipeline was carefully assessed and corrected if needed by a team with long-standing expertise in this area [65,66].

Conclusions

Four main conclusions may be drawn from the present study. First, we show that the overall connectivity profiles of STN- and ALIC-DBS electrodes project to largely different areas in the brain. Second, results of each cohort separately singled out the same fiber tract that was associated with long-term improvement of OCD symptoms when modulated either at the level of the STN or the ALIC. Third, we demonstrated that it is possible to cross-predict clinical improvement of OCD patients across DBS target sites (ALIC / STN) and centers (Cologne / Grenoble). Finally, we show that most if not all literature-defined DBS targets that were used to treat OCD in the past fall along the tract-target identified in the present study.

Methods

Patient Cohorts and Imaging

Thirty-six OCD patients from two different centers were retrospectively enrolled in this study, among them twenty-two patients from University Hospital of Cologne implanted for ALIC DBS and fourteen patients from Grenoble University Hospital who underwent STN DBS surgery. All patients were bilaterally implanted with DBS electrodes 3389, except for three patients from the ALIC cohort, who were implanted with type 3387 electrodes (Medtronic, Minneapolis, Minnesota, US). All patients qualified for DBS surgery based on their diagnoses of treatment-resistant severe OCD [22,28]. Severity of OCD was assessed both pre- and postoperatively with the Yale-Brown Obsessive-Compulsive Scale (Y-BOCS). Postoperative assessment took place 12 months after surgery. Patients' demographic details are provided in Table 1. For detailed demographic and clinical data on the ALIC cohort, see [22] and [67]. All patients gave written informed consent. The protocols were approved by the Ethics Committee of the University of Cologne and the Ethics Committee of Grenoble University Hospital, respectively.

For all patients in both cohorts, high-resolution structural T1-weighted images were acquired on a 3.0-Tesla Philips Healthcare MRI-scanner (Philips Medical Systems, Hamburg, Germany) at the University Hospital of Cologne and the Grenoble University Hospital, respectively, before surgery. Postoperative computer tomography (CT) was obtained in twenty-five patients after surgery to verify correct electrode placement, while eleven patients from the STN cohort instead received postoperative MRI.

DBS Lead Localization and VTA Estimation

DBS electrodes were localized using Lead-DBS software (http://www.lead-dbs.org) as described in [65] and [62]. Briefly, postoperative CT and MRI scans were linearly coregistered to preoperative T1 images using Advanced Normalization Tools (ANTs, http://stnava.github.io/ANTs/) [68]. Subcortical refinement was applied (as a module in Lead-DBS) to correct for brain shift that may have occurred during surgery. Images were then normalized into ICBM 2009b Nonlinear Asymmetric ("MNI") template [33] space using the SyN approach implemented in ANTs [69], with an additional subcortical refinement stage to attain a most precise subcortical alignment between patient and template space ("Effective Low Variance" preset as implemented in Lead-DBS). Of note, this specific method was the top performer for subcortical image registrations in a recent comparative study that involved >10,000 nonlinear warps and a variety of normalization techniques [64]. Both

coregistrations and normalizations were visually reviewed and refined if needed. DBS electrodes were then localized using Lead-DBS and warped into MNI space.

Volumes of Tissue Activated (VTA) were estimated using a finite element method (FEM) as described in [62]. Briefly, a volume conductor model was constructed based on a four-compartment mesh that included gray matter, white matter, electrode contacts and insulated parts. Gray matter was defined by the CIT-168 [31] and DISTAL [32] atlases for the ALIC- and STN-cohorts, respectively. These atlases were specifically adapted or created for use within the Lead-DBS pipeline. The electric field (E-field) distribution was then simulated using an adaptation of the FieldTrip-SimBio pipeline [70] that was integrated into Lead-DBS (https://www.mrt.uni-jena.de/simbio/; http://fieldtriptoolbox.org/) and thresholded at a level of 0.2 V/m [62].

Connectivity Analysis

Structural connectivity between VTA and all other brain voxels was calculated based on a normative connectome as similarly done in previous work [17,22,32,34,59,62]. Specifically, a whole-brain connectome based on state-of-the-art multi-shell diffusion-weighted imaging data from 985 subjects of the Human Connectome Project (HCP) 1200 subjects data release [60] was calculated in each patient using Lead-Connectome. Whole-brain fiber tracts were then normalized into standard space using a multispectral warp based on T1-weighted, T2-weighted, and diffusion-weighted acquisitions using ANTs (using the same “Effective Low Variance” preset implemented in Lead-DBS). In each subject, a total of 6,000 fibers were sampled and aggregated to a joint dataset in standard space. From this, a set of 6,000,000 fibers across 985 HCP subjects were accumulated for analysis in this study. For each of these fiber tracts, a “Fiber T-score” was assigned by associating the fiber tract’s connectivity to VTAs across patients with the clinical outcome (Figure 6). Specifically, (mass-univariate) two-sample t-tests between clinical outcomes in connected and unconnected VTAs were performed for all 6,000,000 tracts. Needless to say, these T-scores were not meant to result in significant results but instead were used to estimate a model that could be used for out-of-sample predictions in the other DBS cohort. The fiber T-scores were then defined as the T-values from these tests and could be positive or negative (since two-sided tests were performed). A high absolute T-score meant that the fiber was strongly discriminative or predictive for clinical outcome. For instance, a tract that was connected exclusively to VTAs in top-responders (and not to VTAs of poor responders) would receive a high positive T-score (termed “Fiber-T-Score” below). In return, a patient would most likely show more pronounced clinical benefit, if her/his VTA was strongly connected to fibers with high positive

T-scores. In figures of this manuscript, fibers were color-coded by their associated T-scores. A schematic overview of the above described method is shown in Figure 6. Only highly predictive fibers were kept (top 20% based on fiber T-scores), which formed the "discriminative fiber set". Based on the discriminative fiber set, the association between the fiber connectivity and the clinical outcome was analyzed. For instance, in the main analysis, a discriminative fiber set was defined exclusively on the ALIC cohort but was then used to predict outcome in patients from the STN cohort (and vice-versa). To do so, the T-scores of connected fibers from the discriminative fiber set were summed up for each patient and this value was correlated with the clinical improvement, as measured by the %-improvement of Y-BOCS scores between preoperative and 12 months postoperative assessments.

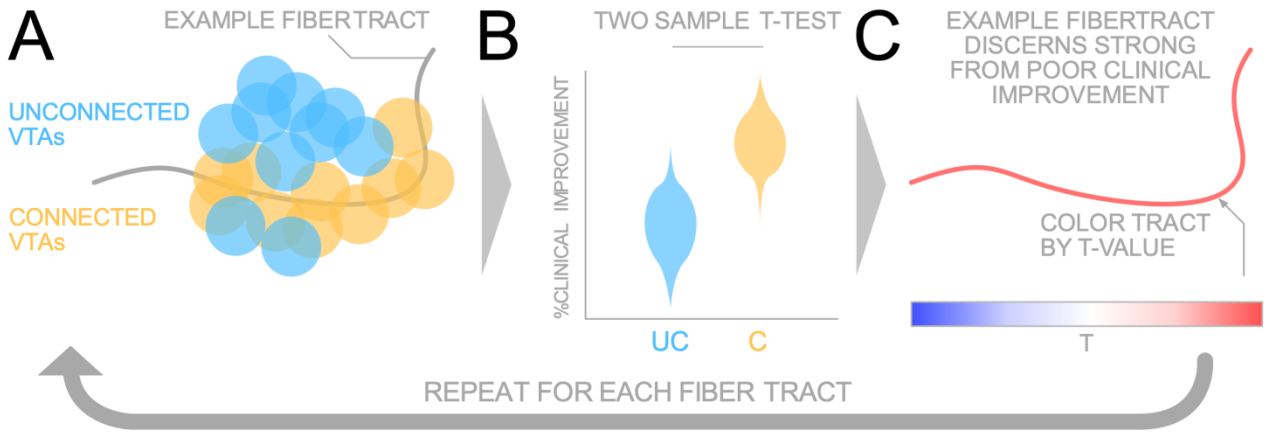

Figure 6. Summary of methods to define a fiber-T-score for each tract. A) For each fiber, VTAs were grouped into either connected (C; yellow) or unconnected (UC; blue) sets across patients. B) Two-sample t-tests between clinical improvements in connected and unconnected VTAs were calculated in a mass-univariate fashion for each fiber tract separately. C) The resulting fiber-T-score of this analysis leads to the "weight" that each fiber is given, as well as the color in visualizations throughout the manuscript. Here, red means that the fiber tract is favorably connected to top responders while blue indicates the opposite (and the saturation of tracts denotes how discriminative they are).

Data and code availability

The DBS MRI datasets generated during and analyzed during the current study are not publicly available due to data privacy regulations of patient data but are available from the corresponding author on reasonable request. All code used to analyze the dataset is available within Lead-DBS /-Connectome software (https://github.com/leaddbs/leaddbs).

References

1. Mallet, L. *et al.* Compulsions, Parkinson's disease, and stimulation. *The Lancet* **360**, 1302–1304 (2002).
2. Chabardès, S. *et al.* Deep Brain Stimulation for Obsessive-Compulsive Disorder: Subthalamic Nucleus Target. *World Neurosurg.* **80**, S31.e1-S31.e8 (2013).
3. Anderson, D. & Ahmed, A. Treatment of patients with intractable obsessive—compulsive disorder with anterior capsular stimulation: Case report. *J. Neurosurg.* **98**, 1104–1108 (2003).
4. Sturm, V. *et al.* The nucleus accumbens: a target for deep brain stimulation in obsessive–compulsive- and anxiety-disorders. *J. Chem. Neuroanat.* **26**, 293–299 (2003).
5. Aouizerate, B. *et al.* Deep brain stimulation of the ventral caudate nucleus in the treatment of obsessive—compulsive disorder and major depression: Case report. *J. Neurosurg.* **101**, 682–686 (2004).
6. Franzini, A. *et al.* Deep-brain stimulation of the nucleus accumbens in obsessive compulsive disorder: clinical, surgical and electrophysiological considerations in two consecutive patients. *Neurol. Sci.* **31**, 353–359 (2010).
7. Greenberg, B. D. *et al.* Three-Year Outcomes in Deep Brain Stimulation for Highly Resistant Obsessive–Compulsive Disorder. *Neuropsychopharmacology* **31**, 2384–2393 (2006).
8. Jiménez-Ponce, F. *et al.* Preliminary Study in Patients With Obsessive-Compulsive Disorder Treated With Electrical Stimulation in the Inferior Thalamic Peduncle. *Oper. Neurosurg.* **65**, ons203–ons209 (2009).
9. Lee, D. J. *et al.* Inferior thalamic peduncle deep brain stimulation for treatment-refractory obsessive-compulsive disorder: A phase 1 pilot trial. *Brain Stimulat.* **12**, 344–352 (2019).
10. Luyten, L., Hendrickx, S., Raymaekers, S., Gabriëls, L. & Nuttin, B. Electrical stimulation in the bed nucleus of the stria terminalis alleviates severe obsessive-compulsive disorder. *Mol. Psychiatry* **21**, 1272–1280 (2016).
11. Nair, G., Evans, A., Bear, R. E., Velakoulis, D. & Bittar, R. G. The anteromedial GPi as a new target for deep brain stimulation in obsessive compulsive disorder. *J. Clin. Neurosci.* **21**, 815–821 (2014).
12. Coenen, V. A. *et al.* The medial forebrain bundle as a target for deep brain stimulation for obsessive-compulsive disorder. *CNS Spectr.* **22**, 282–289 (2017).
13. Maarouf, M. *et al.* Deep Brain Stimulation of Medial Dorsal and Ventral Anterior

Nucleus of the Thalamus in OCD: A Retrospective Case Series. *PLOS ONE* **11**, e0160750 (2016).

14. Borders, C., Hsu, F., Sweidan, A. J., Matei, E. S. & Bota, R. G. Deep brain stimulation for obsessive compulsive disorder: A review of results by anatomical target. *Ment. Illn.* **10**, (2018).
15. Tyagi, H. *et al.* A Randomized Trial Directly Comparing Ventral Capsule and Anteromedial Subthalamic Nucleus Stimulation in Obsessive-Compulsive Disorder: Clinical and Imaging Evidence for Dissociable Effects. *Biol. Psychiatry* (2019). doi:10.1016/j.biopsych.2019.01.017
16. Lozano, A. M. & Lipsman, N. Probing and Regulating Dysfunctional Circuits Using Deep Brain Stimulation. *Neuron* **77**, 406–424 (2013).
17. Horn, A. *et al.* Connectivity Predicts deep brain stimulation outcome in Parkinson disease. *Ann. Neurol.* **82**, 67–78 (2017).
18. Horn, A. The impact of modern-day neuroimaging on the field of deep brain stimulation. *Curr. Opin. Neurol.* **Publish Ahead of Print**, (2019).
19. Schaerer, J., Roche, F. & Belaroussi, B. A generic interpolator for multi-label images. *Insight J.* 950 (2014).
20. Liebrand, L. C. *et al.* Individual white matter bundle trajectories are associated with deep brain stimulation response in obsessive-compulsive disorder. *Brain Stimulat.* **12**, 353–360 (2019).
21. Heilbronner, S. R., Safadi, Z. & Haber, S. N. Neurocircuits commonly involved in psychiatric disorders and their stimulation and lesion therapies. in *Neuromodulation in Psychiatry* 27–48 (John Wiley & Sons, Ltd, 2016). doi:10.1002/9781118801086.ch3
22. Baldermann, J. C. *et al.* Connectivity profile predictive of effective deep brain stimulation in obsessive compulsive disorder. *Biol. Psychiatry* (2019). doi:10.1016/j.biopsych.2018.12.019
23. Akram, H. *et al.* Subthalamic deep brain stimulation sweet spots and hyperdirect cortical connectivity in Parkinson's disease. *NeuroImage* **158**, 332–345 (2017).
24. Middlebrooks, E. H. *et al.* Segmentation of the Globus Pallidus Internus Using Probabilistic Diffusion Tractography for Deep Brain Stimulation Targeting in Parkinson Disease. *Am. J. Neuroradiol.* **39**, 1127–1134 (2018).
25. Vanegas-Arroyave, N. *et al.* Tractography patterns of subthalamic nucleus deep brain stimulation. *Brain* **139**, 1200–1210 (2016).
26. Deuschl, G. *et al.* A Randomized Trial of Deep-Brain Stimulation for Parkinson's Disease. *N. Engl. J. Med.* **355**, 896–908 (2006).

27. Ostrem, J. L. *et al.* Subthalamic nucleus deep brain stimulation in primary cervical dystonia. *Neurology* **76**, 870–878 (2011).
28. Polosan, M. *et al.* Affective modulation of the associative-limbic subthalamic nucleus: deep brain stimulation in obsessive–compulsive disorder. *Transl. Psychiatry* **9**, 73 (2019).
29. Vissani, M., Cordella, R., Micera, S., Romito, L. M. & Mazzoni, A. Spatio-temporal structure of single neuron subthalamic activity in Tourette Syndrome explored during DBS procedures. *bioRxiv* 532200 (2019). doi:10.1101/532200
30. Alkemade, A., Groot, J. M. & Forstmann, B. U. Do We Need a Human post mortem Whole-Brain Anatomical Ground Truth in in vivo Magnetic Resonance Imaging? *Front. Neuroanat.* **12**, (2018).
31. Pauli, W. M., Nili, A. N. & Tyszka, J. M. A high-resolution probabilistic *in vivo* atlas of human subcortical brain nuclei. *Sci. Data* **5**, 180063 (2018).
32. Ewert, S. *et al.* Toward defining deep brain stimulation targets in MNI space: A subcortical atlas based on multimodal MRI, histology and structural connectivity. *NeuroImage* **170**, 271–282 (2018).
33. Fonov, V., Evans, A., McKinstry, R., Almli, C. & Collins, D. Unbiased nonlinear average age-appropriate brain templates from birth to adulthood. *NeuroImage* **47**, S102 (2009).
34. Horn, A. *et al.* Probabilistic conversion of neurosurgical DBS electrode coordinates into MNI space. *NeuroImage* **150**, 395–404 (2017).
35. Mallet, L. *et al.* Subthalamic Nucleus Stimulation in Severe Obsessive–Compulsive Disorder. *N. Engl. J. Med.* **359**, 2121–2134 (2008).
36. Tsai, H.-C., Chen, S.-Y., Tsai, S.-T., Hung, H.-Y. & Chang, C.-H. Hypomania Following Bilateral Ventral Capsule Stimulation in a Patient with Refractory Obsessive-Compulsive Disorder. *Biol. Psychiatry* **68**, e7–e8 (2010).
37. Nuttin, B. J. *et al.* Long-term Electrical Capsular Stimulation in Patients with Obsessive-Compulsive Disorder. *Neurosurgery* **52**, 1263–1274 (2003).
38. Nuttin, B. *et al.* Targeting Bed Nucleus of the Stria Terminalis for Severe Obsessive-Compulsive Disorder: More Unexpected Lead Placement in Obsessive-Compulsive Disorder than in Surgery for Movement Disorders. *World Neurosurg.* **80**, S30.e11-S30.e16 (2013).
39. Bourne, S. K., Eckhardt, C. A., Sheth, S. A. & Eskandar, E. N. Mechanisms of deep brain stimulation for obsessive compulsive disorder: effects upon cells and circuits. *Front. Integr. Neurosci.* **6**, (2012).
40. Figee, M. *et al.* Deep brain stimulation restores frontostriatal network activity in

obsessive-compulsive disorder. *Nat. Neurosci.* **16**, 386–387 (2013).

41. Dunlop, K. *et al.* Reductions in Cortico-Striatal Hyperconnectivity Accompany Successful Treatment of Obsessive-Compulsive Disorder with Dorsomedial Prefrontal rTMS. *Neuropsychopharmacology* **41**, 1395–1403 (2016).
42. Widge, A. S. *et al.* Deep brain stimulation of the internal capsule enhances human cognitive control and prefrontal cortex function. *Nat. Commun.* **10**, 1536 (2019).
43. Mataix-Cols, D. *et al.* Distinct Neural Correlates of Washing, Checking, and Hoarding SymptomDimensions in Obsessive-compulsive Disorder. *Arch. Gen. Psychiatry* **61**, 564–576 (2004).
44. Barcia, J. A. *et al.* Personalized striatal targets for deep brain stimulation in obsessive-compulsive disorder. *Brain Stimulat.* (2018). doi:10.1016/j.brs.2018.12.226
45. Calabrese, E. *et al.* Postmortem diffusion MRI of the human brainstem and thalamus for deep brain stimulator electrode localization. *Hum. Brain Mapp.* **36**, 3167–3178 (2015).
46. Middlebrooks, E. H. *et al.* Structural connectivity–based segmentation of the thalamus and prediction of tremor improvement following thalamic deep brain stimulation of the ventral intermediate nucleus. *NeuroImage Clin.* **20**, 1266–1273 (2018).
47. Choi, K. S. Characterizing structural neural networks in major depressive disorder using diffusion tensor imaging. (Georgia Institute of Technology, 2013).
48. Choi, K. S., Riva-Posse, P., Gross, R. E. & Mayberg, H. S. Mapping the “Depression Switch” During Intraoperative Testing of Subcallosal Cingulate Deep Brain Stimulation. *JAMA Neurol.* **72**, 1252–1260 (2015).
49. Mayberg, H. S. *et al.* Deep Brain Stimulation for Treatment-Resistant Depression. *Neuron* **45**, 651–660 (2005).
50. Schlaepfer, T. E., Bewernick, B. H., Kayser, S., Mädler, B. & Coenen, V. A. Rapid Effects of Deep Brain Stimulation for Treatment-Resistant Major Depression. *Biol. Psychiatry* **73**, 1204–1212 (2013).
51. Schlaepfer, T. E., Bewernick, B. H., Kayser, S., Hurlemann, R. & Coenen, V. A. Deep Brain Stimulation of the Human Reward System for Major Depression—Rationale, Outcomes and Outlook. *Neuropsychopharmacology* **39**, 1303–1314 (2014).
52. Follett, K. A. *et al.* Pallidal versus Subthalamic Deep-Brain Stimulation for Parkinson’s Disease. *http://dx.doi.org/10.1056/NEJMoa0907083* (2010). doi:10.1056/NEJMoa0907083
53. Odekerken, V. J. *et al.* Subthalamic nucleus versus globus pallidus bilateral deep brain stimulation for advanced Parkinson’s disease (NSTAPS study): a randomised

controlled trial. *Lancet Neurol.* **12**, 37–44 (2013).

54. Odekerken, V. J. J. *et al.* GPi vs STN deep brain stimulation for Parkinson disease: Three-year follow-up. *Neurology* **86**, 755–761 (2016).
55. Darby, R. R., Horn, A., Cushman, F. & Fox, M. D. Lesion network localization of criminal behavior. *Proc. Natl. Acad. Sci. U. S. A.* **115**, 601–606 (2018).
56. Joutsa, J., Horn, A., Hsu, J. & Fox, M. D. Localizing parkinsonism based on focal brain lesions. *Brain* **141**, 2445–2456 (2018).
57. Joutsa, J. *et al.* Identifying therapeutic targets from spontaneous beneficial brain lesions. *Ann. Neurol.* **84**, 153–157 (2018).
58. Weigand, A. *et al.* Prospective Validation That Subgenual Connectivity Predicts Antidepressant Efficacy of Transcranial Magnetic Stimulation Sites. *Biol. Psychiatry* **84**, 28–37 (2018).
59. Neumann, W.-J. *et al.* Functional segregation of basal ganglia pathways in Parkinson's disease. *Brain* **141**, 2655–2669 (2018).
60. Glasser, M. F. *et al.* The Human Connectome Project's neuroimaging approach. *Nat. Neurosci.* **19**, 1175–1187 (2016).
61. Petersen, M. V. *et al.* Probabilistic versus deterministic tractography for delineation of the cortico-subthalamic hyperdirect pathway in patients with Parkinson disease selected for deep brain stimulation. *J. Neurosurg.* **126**, 1657–1668 (2017).
62. Horn, A. *et al.* Lead-DBS v2: Towards a comprehensive pipeline for deep brain stimulation imaging. *NeuroImage* **184**, 293–316 (2019).
63. Husch, A., V. Petersen, M., Gemmar, P., Goncalves, J. & Hertel, F. PaCER - A fully automated method for electrode trajectory and contact reconstruction in deep brain stimulation. *NeuroImage Clin.* **17**, 80–89 (2017).
64. Ewert, S. *et al.* Optimization and comparative evaluation of nonlinear deformation algorithms for atlas-based segmentation of DBS target nuclei. *NeuroImage* **184**, 586–598 (2019).
65. Horn, A. & Kühn, A. A. Lead-DBS: A toolbox for deep brain stimulation electrode localizations and visualizations. *NeuroImage* **107**, 127–135 (2015).
66. Schönecker, T., Kupsch, A., Kühn, A. A., Schneider, G.-H. & Hoffmann, K.-T. Automated Optimization of Subcortical Cerebral MR Imaging−Atlas Coregistration for Improved Postoperative Electrode Localization in Deep Brain Stimulation. *Am. J. Neuroradiol.* **30**, 1914–1921 (2009).
67. Huys, D. *et al.* Open-label trial of anterior limb of internal capsule–nucleus accumbens deep brain stimulation for obsessive-compulsive disorder: insights gained. *J. Neurol.*

Neurosurg. Psychiatry jnnp-2018-318996 (2019). doi:10.1136/jnnp-2018-318996

68. Avants, B. B., Tustison, N. & Song, G. Advanced normalization tools (ANTS). *Insight J* **2**, 1–35 (2009).
69. Avants, B. B., Epstein, C. L., Grossman, M. & Gee, J. C. Symmetric Diffeomorphic Image Registration with Cross-Correlation: Evaluating Automated Labeling of Elderly and Neurodegenerative Brain. *Med. Image Anal.* **12**, 26–41 (2008).
70. Vorwerk, J., Oostenveld, R., Piastra, M. C., Magyari, L. & Wolters, C. H. The FieldTrip-SimBio pipeline for EEG forward solutions. *Biomed. Eng. OnLine* **17**, 37 (2018).

Acknowledgements

This work was supported by the German Research Foundation (Deutsche Forschungsgemeinschaft, Emmy Noether Stipend 410169619 to AH, KFO 247 to AAK and KFO 219 to JK).

Author contributions

A. H., N.L. and A.A.K. conceptualized the study. A.H. and N.L. developed the software pipeline used, analyzed data and wrote the manuscript. J.C.B. conceptualized the study, acquired patient data and revised the manuscript. S.T. co-wrote the manuscript. A.K., acquired data and revised the manuscript. S.C. V.V.V. M.P. J.K. acquired patient data and revised the manuscript. G.J.B.E., A.B., and A.M.L. processed and analyzed human connectome data and revised the manuscript.

Competing interests

A.H. reports one-time lecture fee for Medtronic. A.A.K. reports personal fees and non-financial support from Medtronic, personal fees from Boston Scientific, grants and personal fees from Abbott outside the submitted work. A.M.L. is consultant for Medtronic, Abbott and Boston Scientific. M.P. has received honoraria for lecturing from the Movement Disorder Society, Medtronic, research support from Boston Scientific. S.C. is consultant for Medtronic, Boston Scientific and Zimmer Biomet. JK has received financial support for investigator-initiated trials from Medtronic. A.B., A.K., G.J.B.E., J.C.B., N.L., S.T. and V.V.V. have nothing to disclose.

Materials & Correspondences

Correspondence and material requests should be addressed to Ningfei Li (ningfei.li@charite.de)

Supplementary Material

Video S1: Exemplary use-case of postoperative DBS-programming guided by the tract-atlas released within Lead-DBS software